

PAPER • OPEN ACCESS

Experimental study on heat transfer through a few layers of multilayer insulation from 300 K to 4.2 K

To cite this article: Zhanguo Zong *et al* 2017 *IOP Conf. Ser.: Mater. Sci. Eng.* **171** 012089

View the [article online](#) for updates and enhancements.

Related content

- [Demonstration of Hybrid Multilayer Insulation for Fixed Thickness Applications](#)
W L Johnson, J E Fesmire and K W Heckle

- [Preliminary Design of the Vacuum System for FAIR Super FRS Quadrupole Magnet Cryostat](#)
J Akhter, G Pal, A Datta et al.

- [Thermal Performance Testing of Cryogenic Multilayer Insulation with Silk Net Spacers](#)
W L Johnson, D J Frank, T C Nast et al.

Experimental study on heat transfer through a few layers of multilayer insulation from 300 K to 4.2 K

Zhanguo Zong, Norihito Ohuchi, Kiyosumi Tsuchiya, Yasushi Arimoto and Hiroshi Yamaoka

High Energy Accelerator Research Organization, 1-1 Oho, Tsukuba, Ibaraki, 305-0801, Japan

zhanguo.zong@kek.jp

Abstract. The final focusing magnet system at the SuperKEKB interaction region has been designed under stringent space constraints and consists of 8 main Superconducting (SC) quadrupole magnets, 4 compensation SC solenoids, and 43 SC correction coils. SC correction coils are directly wound on the inner containment tubes of liquid helium (LHe) vessels, which serve as support bobbins for SC cables. Beam pipes, which are kept at room temperature (~300 K), are inserted into the cold bores of the vessel inner tubes. Between them, the minimal radial gaps are only 3.5 mm. Heat transfer from the warm beam pipes causes the raised operation temperatures of SC cables and increases heat leaks into cryostats. Multilayer insulation (MLI) is adopted to reduce heat flux in the narrow gaps. MLI performance as a function of the layer number was studied with a vertical anti-cryostat of dedicated design. The measurements were carried out by a calorimeter of thermal conduction and a modified LHe boil-off method. This paper presents the cryogenic measurement system and discusses the experimental results for the cryostats of the SuperKEKB final focusing SC magnets.

1. Introduction

The SuperKEKB is the upgraded accelerator of KEKB and its target luminosity is $8 \times 10^{35} \text{ cm}^{-2}\text{s}^{-1}$, which is 40 times higher than that of KEKB [1]. The accelerator design is based on the nano-beam scheme and focusing beams to a vertical beam size of about 50 nm at interaction point (IP) is performed by Superconducting (SC) quadrupole doublets of each beam line. The final focusing magnet system consists of eight main SC quadrupole magnets (QCS), four compensation SC solenoids (ES), and 43 SC correction coils [2]. The SC magnets are assembled into two cryostats, located at the left and right sides of the accelerator IP, respectively.

The two cryostats are cantilevered inside the detector, Belle-II, and the outer sizes of the cryostats are constrained by the components of the detector. As the result, the SC magnets and cryostats has been designed under stringent space constraints, especially at the radial direction. The inner radii of the cryostats are limited by the dimensions of beam pipes, which are required by the accelerator beam optics. To fit the extremely tight radial spaces, the SC correction coils with maximum currents of about 60 A are directly wound to the inner containment tubes of liquid helium (LHe) vessels, using the BNL Direct Wind technique [3]. Figure 1 shows the cross sections of the QC1P/1E magnets, which are located at the closest positions to IP along each beam line. The radial spaces for the SC corrector coils are between the LHe vessel tubes and the inner windings of the main quadrupole coils. The inner tubes serve as the support bobbins of SC corrector coils. The beam pipes are kept at room temperature



Content from this work may be used under the terms of the [Creative Commons Attribution 3.0 licence](https://creativecommons.org/licenses/by/3.0/). Any further distribution of this work must maintain attribution to the author(s) and the title of the work, journal citation and DOI.

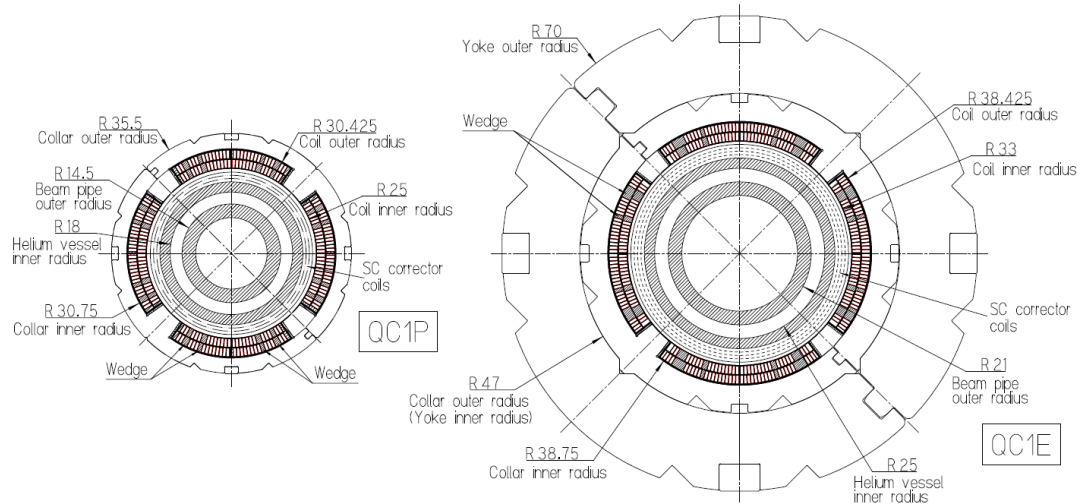


Figure 1. Cross sections of the QC1P/1E magnets.

(~300 K) and are inserted into the cold bores of the LHe vessels. In table 1, the outer radii of the beam pipes and the inner radii of the coil bobbins are listed for all the SuperKEKB final focusing SC magnets. For each quadrupole magnet, the dimensions of the LHe vessel inner tubes are different in order to accommodate the variations of the beam pipes. The radial gaps between the warm beam pipes and cold coil bobbins are 3.5 mm, 4 mm and 6 mm, respectively.

Table 1. Dimensions of beam pipes and coil bobbins of the QCS magnets.

Item	QC1P	QC1E	QC2P	QC2E
Outer radius of beam pipe	14.5	21	39	44
Inner radius of coil bobbin	18.0	25	45	50
Gap for MLI	3.5	4	6	6

Heat transfer from the warm beam pipes causes the elevated operation temperatures of the innermost SC correction coils and increases heat leaks into the cryostats. Multilayer insulation (MLI) is wrapped around the warm beam pipes in the gaps to reduce heat leaks as MLI has the best performance of all thermal insulations [4]. The actual performance of MLI depends on a few parameters hard to control, such as layer density, compressive loading, and total layers. Extensive studies and experimental measurements are necessary to evaluate the thermal performance of MLI and to obtain application experiences and fabrication details in specific circumstances. A vertical cryostat with doubled LHe vessels was designed and the warm bore with an evacuated gap to accommodate variable MLI layers was inserted into LHe in the vertical cryostat. Heat transfer from the warm bore, through a few MLI layers to LHe, was measured by a calorimeter of thermal conduction and a modified LHe boil-off method. In this paper, the measurement system is presented and heat leak estimation using the measured results is described for cryogenic system of the SuperKEKB final focusing SC magnets.

2. Measurement system

A schematic illustration of the vertical cryostat for measuring the MLI performance is shown in figure 2. The vertical cryostat was equipped with the vacuum chamber for MLI and liquid nitrogen intermediate interception (not shown in figure 2). In addition, the doubled LHe vessels were designed to exclude the conduction heat loss from the wall of the LHe vessel. The cryostat vessel had a diameter of 300 mm and served as the outer LHe container. The inner LHe vessel had a diameter of 210.3 mm. The inner LHe vessel was immersed in the LHe of the outer container and during measuring the LHe level of the inner vessel was lower than that of the outer LHe vessel. The inner LHe was evaporated only by heat leaks from the warm bore.

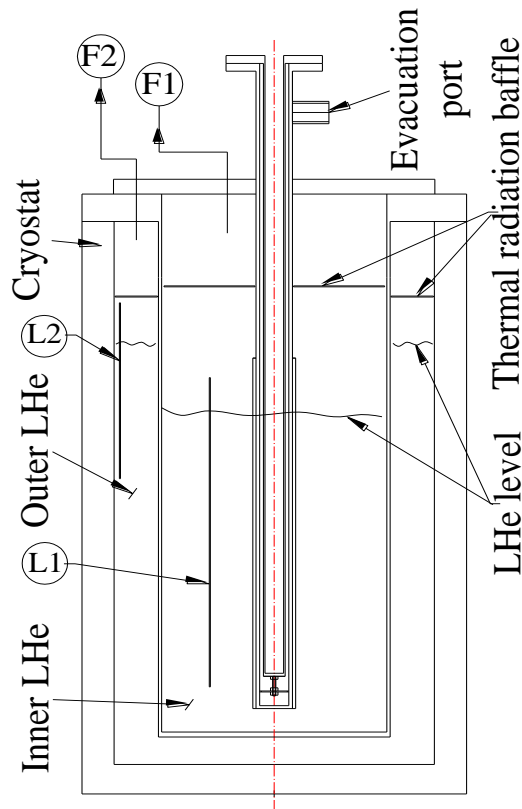


Figure 2. Schematic illustration of the vertical cryostat.

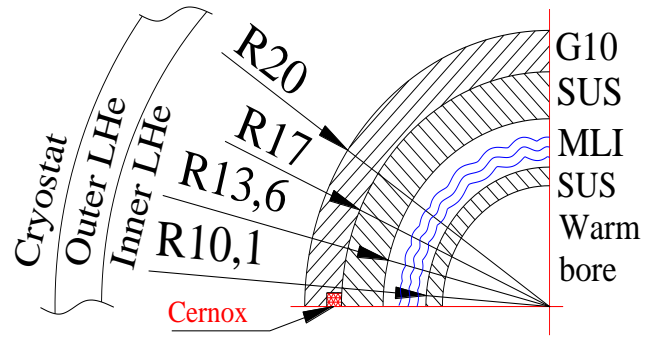


Figure 3. Quarter of the warm bore cross section in the vertical cryostat.

A quarter cross section of the warm bore with MLI at the narrow gap is shown in figure 3, and the LHe vessels are schematically sketched. The narrow gap was designed with a dimension of 3.5 mm ($R=13.6$ mm to $R=10.1$ mm), which was the same as those of the QC1P magnets. At the top of the 1.4 m long gap, the SUS pipes were sealed by a common O-ring for simple mounting requirements to change MLI layers. At the pipe bottom, a SUS plate with four sharp feet was utilized to keep the two SUS pipes concentric. Several layers of MLI were wrapped around the innermost SUS pipe ($R=10.1$ mm) layer by layer.

The inner bore of the innermost pipe was kept at room temperature by blowing nitrogen gas of about 300 K. The cold tube surface (the outer radius of $R=17$ mm) was covered by a G10 cylinder of 900 mm long, and was inserted in LHe. Three calibrated Cernox™ temperature sensors were attached to the surface (at $R=17$ mm) to measure its temperature. The inner LHe bath temperature was also measured by a Cernox™ sensor. The temperature difference over the G10 cylinder wall functioned as the calorimeter of thermal conduction.

When the outer LHe level was higher than the inner LHe level, heat leaks from the cryostat background were able to be intercepted by the outer LHe. Heat leaks only from the warm bore could reach the inner LHe and were able to be measured by the evaporated helium vapor flow (F1 in figure 2).

As the space between two SUS tubes was evacuated to a vacuum level of 10^{-4} Pa before cooling and was kept at 10^{-5} Pa levels during measuring, the contribution by conduction of residual gas was neglected [5]. The monitored helium vapor flow (F1) was because of the thermal conduction of the support plate at the bottom and the thermal radiation through MLI layers. The support plate was designed with thin and sharp feet to increase the resistance of thermal conduction. As the bottom side of the pipes was always immersed in LHe during measuring, the surrounding thermal conditions did

not change. The thermal conduction of the support plate to LHe was constant and was calculated with an AnsysTM simulation. It was about 0.13 W.

Heat leaks because of the thermal radiation through MLI layers were firstly received by the SUS tube ($R=13.6$ mm) and were conducted to helium environment along the radial direction of the SUS tube and G10 cylinder. Heat leaks absorbed by LHe were proportional to the length of the SUS tube or the G10 cylinder, immersed in LHe. Correspondingly, the monitored helium vapor flow had a linear relationship with the inner LHe level. In this measurement, thermal radiation through MLI layers was measured with the modified method of LHe boil-off.

3. Measured results

In this study, the MLI layer was from the MLI blankets for the KEK STF cryomodule [6][7] and one MLI layer was defined with one aluminized shield and one spacer layer. One MLI layer was cut to a rectangle with the length of about 1.0 m. The width was 5 mm wider than the circumference of the inner pipe ($R=10.1$ mm) for an overlap joint. The MLI layers were wrapped around the inner pipe layer by layer. Each layer was fixed in the azimuthal direction with several aluminum tapes along the pipe. Considerable attention had been given to confirm no compressive load in the radial direction and no large scale crinkling to form thermal shorts to the cold tube in LHe. As MLI layers were light, there was no support point along the longitudinal direction.

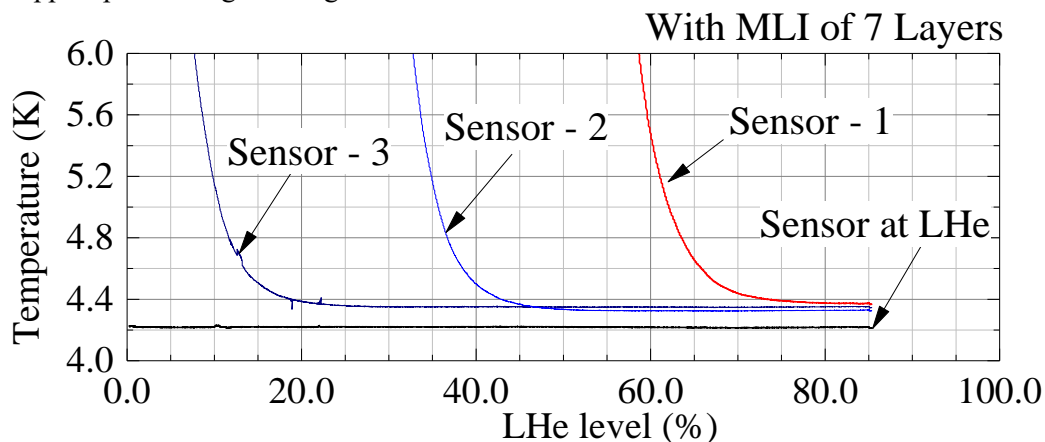


Figure 4. Temperature evolutions of sensors with the LHe level.

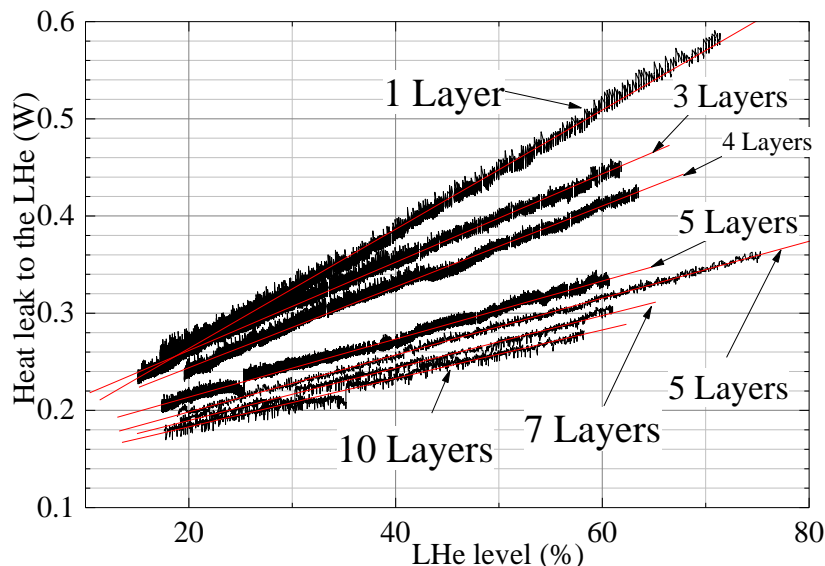


Figure 5. Heat leak to the inner LHe versus LHe level and fitting.

Before cooling, the gap with MLI layers was evacuated for about 24 hours and reached to a vacuum level of 10^{-4} Pa. The cryostat was firstly pre-cooled with liquid nitrogen for thermal stability about 24 hours before LHe transferring. After gas displacement, the cryostat was filled with LHe to the heights upper than the three Cernox™ sensors. Figure 4 shows the monitored temperature evolutions with the LHe level. The temperatures of three sensors (Sensor - 1, - 2 and - 3) were constant and stable when they were all immersed in LHe. At the LHe level of 80 %, their average temperature was 4.351 K with a small standard deviation of 0.023 K. By comparison with LHe temperature (Sensor in the LHe bath, 4.218 K), the temperature difference of 0.133 K was concluded over the G10 cylinder wall. The heat leak was calculated with the G10 material thermal conductivity of 0.072 W/m-K and is about 4.68 W/m² (at the inner surface (R=13.6 mm)).

During measuring, the evaporated helium vapor flow was monitored by a precise thermal flow meter. The corresponding heat leak was the product of the monitored mass flow rate and the latent heat of LHe. The heat leaks of different MLI layers are plotted in figure 5. By linear fitting, the line slopes are heat leaks per unit length due to heat transfer through MLI in the gap. In the cryogenic measurement system, the LHe level meter was 859.6 mm and the corresponding heat flux per meter was calculated. For the measurement with 7 layers of MLI, the fitting slope was 0.0025 W/%. The heat flux per unit length was calculated and was 0.291 W/m. Heat flux density at the inner surface (R=13.6 mm) of the cold tube was about 3.4 W/m². The fitting constant was about 0.15 W, which agrees with the numerical simulation of the support plate.

The measured variations of MLI performance with different layers are summarized in figure 6. When MLI is less than 5 layers, heat flux has a fast reduction with increasing MLI layers. More than 5 layers, the heat flux density are less than 5 W/m². For the measurements of MLI more than 5 layers, the temperature differences, ΔT , between the liquid helium bath and the surface of the SUS tube are shown in figure 6 as a reference to the LHe boil-off method.

In the cryostats of the SuperKEKB final focusing SC magnets, the total area against the warm beam pipes are about 0.86 m². With a heat flux density of 5 W/m², the total heat leak due to thermal radiation is about 4.3 W. The temperatures of SC cables of SC corrector coils are elevated less than 0.2 K.

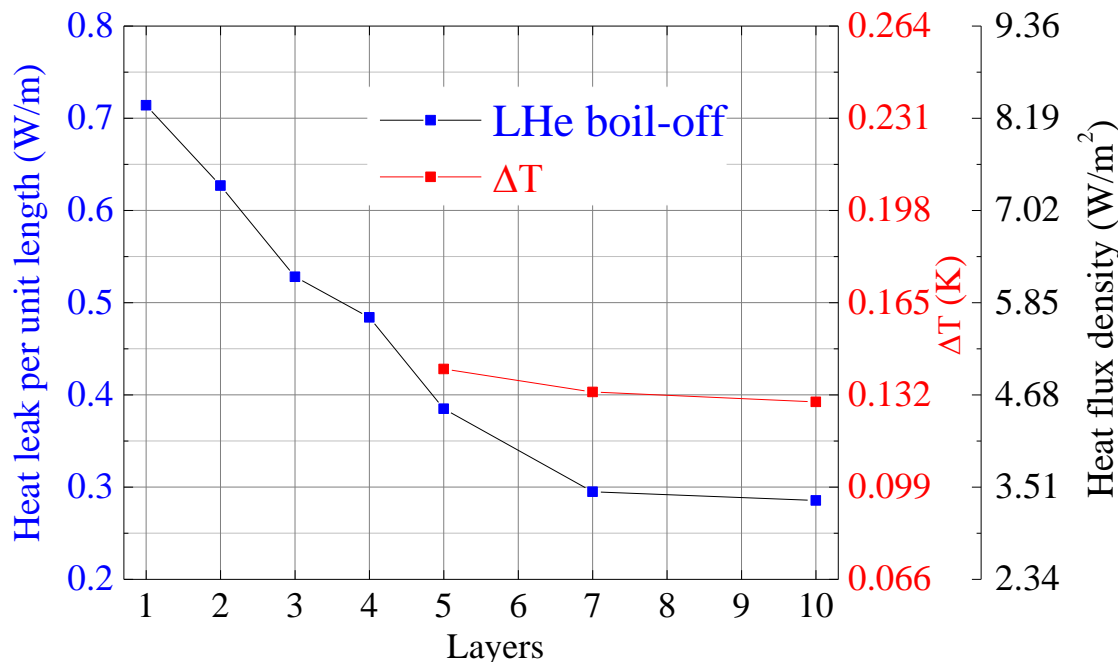


Figure 6. Variations of the measured heat leaks with different layers of MLI.

4. Conclusion

With the dedicated design of the vertical cryostat of doubled LHe vessels, heat transfer through a few layers of MLI from 300 K to 4.2 K (LHe temperature) was experimentally measured, with the calorimeter of thermal conduction and the modified LHe boil-off method. The trend of the MLI performance with different total layers was outlined for estimating the heat leak through the vacuum gaps of the SuperKEKB final focusing SC magnet cryostats. With more than 5 layers, heat flux density to the cold bobbin could be reduced to below 5 W/m² and the total heat leak due to thermal radiation could be less than 4.3 W.

References

- [1] Ohuchi N et al 2014 Construction status of SuperKEKB *Proceedings of the IPAC2014 (Dresden Germany)* pp 1877–1879
- [2] Ohuchi N et al 2013 Design of the Superconducting Magnet System for the SuperKEKB Interaction Region *Proceeding of the PAC2013 (Pasadena CA USA)* pp 759–761
- [3] Parker B et al 2012 Direct wind superconducting corrector magnets for the SuperKEKB IR *Proceedings of the IPAC2012 (New Orleans Louisiana USA)* pp 2191–2193
- [4] Thomas M Flynn 2005 *Cryogenic Engineering* (Second Edition Louisville, CO, U.S.A)
- [5] Wang X L et al 2014 Thermal performance analysis and measurements of the prototype cryomodules of European XFEL accelerator – Part I *Nuclear Instruments and Methods in Physics Research A* vol 763 pp 701–710
- [6] Ohuchi N et al 2010 Experimental study of thermal radiation shield for ILC cryomodule *Proceeding of ICEC23 (Wroclaw Poland)*
- [7] Ohuchi N et al 2012 Study of thermal radiation shields for the ILC Cryomodule *Advances in Cryogenic Engineering (Washington USA)* pp 929–936.